BIOLOGY OF REPRODUCTION **82,** 930–939 (2010)
Published online before print 3 February 2010.
DOI 10.1095/biolreprod.109.081679

USP8, a Regulator of Endosomal Sorting, Is Involved in Mouse Acrosome Biogenesis Through Interaction with the Spermatid ESCRT-0 Complex and Microtubules[1]

Giovanna Berruti,[2,3] Michela Ripolone,[3] and Michela Ceriani[4]

Laboratory of Cellular and Molecular Biology of Reproduction,[3] Department of Biology, University of Milano, Milano, Italy
Department of Biotechnology and Biosciences,[4] University of Milano-Bicocca, Milano, Italy

ABSTRACT

Ubiquitin-specific peptidase 8 (USP8) is a deubiquitinating enzyme that works as a regulator of endosomal sorting and vesicle morphology in cultured cells. Its function in vivo is, however, unknown as *USP8* gene deletion leads to embryonic lethality. Previously, we have shown that USP8 is highly expressed in male germ cells. These cells develop a peculiar acidic vesicle that is indispensable for fertilization, the acrosome; USP8 might be involved in vivo in acrosomogenesis. The objective of this study was to test this hypothesis by determining if selective components of the early endosomal machinery interact functionally with USP8 during acrosomogenesis using protein-protein interaction assays and double/triple immunolabeling. Moreover, by exploiting the characteristic of USP8 that exhibits a microtubule interacting and trafficking/transport (MIT) domain, we verified whether USP8 effectively associates with spermatid microtubules by microtubule cosedimentation and binding assays. USP8 was able to interact with spermatid ESCRT-0 (endosomal-sorting complex required for transport-0) and microtubule structures; USP8/ESCRT-0-labeled vesicles, monitored by fluorescence microscopy, were found to contribute to acrosome formation while USP8 can directly link, via its MIT domain, the labeled vesicles/developing acrosome to microtubules, which could favor both acrosome assembly and shaping. VPS54, the vacuolar-sorting protein responsible for early endocytic retrograde transport, was here detected for the first time in male germ cells; VPS54 followed the intracellular route of USP8/ESCRT-0-labeled vesicles during acrosomogenesis. We concluded that in vivo USP8 has a role strongly associated with acrosome biogenesis and that the early endosome pathway is significantly involved in the process, which suggests that the acrosome could be a novel lysosome-related organelle.

acrosome, acrosome biogenesis, early endosome, endosomes, spermatid, spermatogenesis, STAM2, USP8, VPS54

INTRODUCTION

The deubiquitinating enzyme USP8 (ubiquitin-specific peptidase 8; previously named UBPy, ubiquitin-specific processing protease-y) was originally identified as a putative protein encoded by a cDNA expressed in human myeloblasts (hUBPy) [1] and then found, through independent yeast two-hybrid screenings of mouse libraries, as a protein (mUBPy) that interacts with STAM2 (also known as Hbp) [2] and the Ras-guanine nucleotide exchange factor CDC25/RasGRF1 [3]. Highly conserved homologues of USP8 have been recently identified in other mammals such as rat (GenBank accession number NP 001099972), macacus (XP 001114466), and ox (NP 001069594), as well as in monotremes (XP 001507996), birds (XP 413830), and amphibians (NP 001080551). Moreover, USP8 shares significant homology with deubiquitinating enzymes found in echinoderms, insects, and fungi, in particular with Doa4 of *Saccharomyces cerevisiae* [4]. Thus, *USP8* represents an evolutionarily conserved gene family, and the function of the *USP8* gene product itself might be evolutionarily conserved. In vitro studies exploiting the overexpression of recombinant wild-type mouse USP8 and/or dominant negative USP8 mutants reveal that USP8 plays multiple roles at the endosomal compartment, from the crucial function in the down-regulation of tyrosine kinase membrane receptors [5–7] to the protection of proteins of the endosomal transport machinery from proteasomal degradation [8] and the control of the number and size of endocytic vesicles [5, 9]. *USP8* deletion in mice results in embryonic lethality while conditional mouse mutants for the induced deletion of *USP8* die 4–6 days after administration of the inducer [9]. Consequently, notwithstanding the fact that there are more than 90 predicted active deubiquitinating enzymes in the mammalian genome [10], USP8 function in vivo cannot be replaced by other deubiquitinases.

Since alternative *USP8* animal models, more suitable for understanding its role in vivo, are not presently available, some insight into its function may be gained from the cells that physiologically express the deubiquitinase in high amounts, that is, spermatogenic and neuronal cells [3, 11, 12]. Both of these cell types are characterized by a highly functional polarization of the cell body, and their cell functionality is thought to be strictly dependent on vesicular trafficking and related, ubiquitin-dependent, sorting of protein cargoes [13–15]. The number and position of ubiquitin molecules bound to lysine residues of a target protein are, in fact, an important signal for directing the subcellular localization and intracellular traffic of the protein cargo, and the ubiquitin-specific proteases like USP8 are critical in defining the trimming of the ubiquitin moiety [16].

Moreover, neurons and sperm possess additional, cell-specific vesicular organelles: the neuronal-signaling endosome [17] and the sperm acrosome. The sperm acrosome is an acidic secretory vacuole, considered to be indispensable at fertilization, whose nature and origin, however, have not yet been clearly defined. Originally described as a modified lysosome [18], the acrosome has been then reported as a direct Golgi-derived secretory vesicle [19, 20], and some studies have even argued against its lysosomal/endosomal origin [21]. More recently, however, the concept of it being a Golgi-derived

[1]Supported by Fondo Interno per la Ricerca Scientifica-Tecnologica 2007–2008 University of Milano and PRIN 2008 to G.B.
[2]Correspondence: Giovanna Berruti, Department of Biology, University of Milano, Via Celoria 26, 20133 Milano, Italy. FAX: 39 02 50314802; e-mail: giovanna.berruti@unimi.it

Received: 25 September 2009.
First decision: 25 October 2009.
Accepted: 27 January 2010.

eISSN: 1529-7268 http://www.biolreprod.org
ISSN: 0006-3363

organelle has been revisited [22, 23], and its lysosomal origin is being once again considered [24, 25]. Significantly, previously unidentified vesicle membrane proteins working at the plasma membrane/early endosome level, as AFAF [26] and DYDC1 [27], or as a regulator of lysosomal delivery, as SPE-39 [28], have been recently shown to be involved in acrosomogenesis. So, at present, experimental evidence indicates that there are at least two sources of vesicular transport to the developing acrosome, one derived from the Golgi and one from the plasma membrane, as already suggested when the outer acrosomal membrane was proposed as another plasma membrane [29]. The genesis of the acrosome remains an issue of some importance to be clarified in its details; in mammals, spermatozoa lacking a true acrosome are infertile [30]. In this context, we have addressed questions related to mouse USP8 and the early endosome/vesicular system in spermatogenic cells with particular attention to differentiating spermatids, the cells where acrosomogenesis takes place.

MATERIALS AND METHODS

Animals

Testes were collected from 3- to 4-mo-old CD1 male mice (Charles River, Calco, Italy). Handling of mice and experimental procedures were reviewed and approved by the Ethical Committee of the University of Milano and were performed in accordance with the Guidelines for the Care and Use of Laboratory Animals promulgated by the Italian Minister of Health, DL 27 January 1992 No. 116.

Antibodies

Primary antibodies used in this study were: rabbit anti-mouse USP8 described previously [3]; rabbit anti-STAM2 [31] (a gift of Dr. Naomi Kitamura, Yokohama, Japan); goat anti-STAM (Santa Cruz Biotechnology, Santa Cruz, CA); rabbit anti-HGS (Santa Cruz Biotechnology); rabbit anti-VPS54 [32] (a gift of Dr. Frank Stenner, Zurich, Switzerland); mouse polyclonal anti-VPS54 (Abnova, Taipei, Taiwan); rabbit or mouse anti-GST (Santa Cruz Biotechnology); mouse monoclonal anti-EEA1 (BD Transduction Laboratories, Mississauga, ON, Canada); mouse monoclonal anti-β-tubulin (Sigma-Aldrich Chemical Company, St. Louis, MO). Secondary anti-rabbit, anti-goat, and anti-mouse horseradish peroxidase-linked antibodies were from GE Healthcare (Buckinghamshire, U.K.); secondary Alexa 488- and Alexa 568-conjugated anti-rabbit IgG, anti-goat IgG and anti-mouse IgG antibodies were from Invitrogen (Leek, The Netherlands).

Isolation of Spermatogenic Cells

Spermatogenic cells were isolated in RPMI-1640 (Sigma) medium from adult mouse testes by sequential enzymatic treatments using standardized methodology [33, 34]. Spermatid-enriched fractions were essentially obtained by mechanical dissociation of seminiferous tubules.

RT-PCR Analysis

Total RNA was extracted from testes and/or isolated spermatogenic cells using TRIzol reagent (Invitrogen) according to the manufacture's instructions. Complementary DNA was synthesized from 1 μg of total RNA by using Invitrogen SuperScript III First-Strand Synthesis System for RT-PCR. The cDNA was then amplified by using either mouse *Stam2*-specific primers (forward 5′-CTCCTGGGGCAGTCCCTGGC-3′ and reverse 5′-TCCAGAAC ACAGCATCCGGTTTGCC-3′) that amplify a 795-bp STAM2 fragment or mouse *Hgs*-specific primers (forward 5′-AGCGGCCCCTTTAGTGAGTA-3′ and reverse 5′-ATGCTGGGATCTGCTGTTGT-3′) that amplify a 725-bp HGS fragment. After 35 cycles of PCR, the reactions were analyzed on a 1.5% agarose-ethidium bromide gel. Images were captured with Polaroid film under ultraviolet light.

Subcellular Protein Fractionation and Immunoblotting Analysis

One-percent Triton X-100-soluble protein lysates and hypotonic protein extracts from freshly isolated spermatogenic cells were obtained as described [33]. To separate cytosolic and membrane particulate fractions, the hypotonic extract from postnuclear supernatant was spun at 100 000 × *g* for 1 h at 4°C. The resulting supernatant is the cytosolic fraction while the pellet is the membrane fraction [33]. The membrane fraction was solubilized by incubation in 2X SDS sample buffer for 15 min at 37°C and centrifuged; the supernatant was recovered. Protein concentrations were determined using Bio-Rad DC protein assay (Bio-Rad, Hercules, CA). Proteins were separated by SDS-PAGE and transferred to a nitrocellulose membrane (Hybond-ECL, GE Healthcare) to be immunoprobed with the appropriate primary antibody. This was followed by treatment with the appropriate secondary, horseradish peroxidase-conjugated, immunoglobulins (IgGs) (GE Healthcare) and a chemiluminescence detection system (Pierce Chemical, Rockford, IL).

Coimmunoprecipitation Assay

Freshly prepared protein lysates, first preadsorbed to protein A-Sepharose beads (Sigma-Aldrich) and then clarified by centrifugation, were processed for immunoprecipitation assays. Clarified lysates (100 μg protein) were mixed with the appropriate antibody and incubated for 2 h, at 4°C, on a rotating platform, followed by the addition of protein A-Sepharose beads suspended in the lysate buffer, including a mixture of complete protease-inhibitor and phosphatase-inhibitor cocktails (Sigma-Aldrich) for a further 1 h. Preimmune serum was used for the control samples. After extensive washing (three times in 0.5% Triton X-100 in 50 mM Tris-HCl, pH 7.5, 100 mM NaCl, and 1 mM ethylenediaminetetraacetic acid [EDTA], and once in 50 mM Tris-HCl, pH 7.5, 100 mM NaCl, and 1 mM EDTA), the immunocomplexes were eluted by boiling in 2X SDS sample buffer to be then resolved by SDS-PAGE. After the blot transfer, the nitrocellulose membrane was incubated in the presence of the appropriate antibodies.

Production and Purification of Recombinant Proteins

The following constructs for expression of glutathione S-transferase (GST) fusion proteins, namely, were used: GST-USP8$_{542\text{-}1080}$ (kindly provided by Dr. E. Martegani, University of Milano-Bicocca, Italy), GST-USP8$_{1–438}$, and GST-USP8$_{1–133}$ (kindly provided by Dr. S. Urbé, School of Biomedical Sciences, Liverpool, U.K.), and GST-USP8$_{542–660}$ [3]. GST-USP8$_{542\text{-}1080}$ fusion construct contains the second SH3-binding motif (amino acids 666–731) of USP8 [2] while GST-USP8$_{542–660}$ contains the Ras-GRF1-binding domain [3]; GST-USP8$_{1–438}$ and GST-USP8$_{1–133}$ fusion constructs contain the USP8 microtubule interacting and trafficking/transport (MIT) domain (amino acids 1–133) [35]. Protein production, including GST alone to be used as a positive control, was induced in *Escherichia coli* DH5 alpha cells grown in Luria-Bertani medium (Life Technologies, Carlsbad, CA) supplemented with ampicillin, using 0.1 mM isopropyl-1-thio-beta-D-galactopyranoside (Sigma-Aldrich) for 4 h at 25°C. The bacteria were lysed by sonication in ice-cold 50 mM Tris-HCl, pH 7.4, 50 mM NaCl, 5% (v/v) glycerol, 0.5 mM dithiothreitol (DTT), plus a complete protease inhibitor cocktail (Sigma-Aldrich) and 1% Triton X-100 (final concentration). The lysates were clarified by centrifugation at 25 000 × *g* for 15 min at 4°C, and the GST fusion proteins were affinity-purified by batchwise incubation with glutathione-Sepharose beads (GE Healthcare) at 4°C according to manufacturer's instructions. The proteins were eluted with 20 mM glutathione (Sigma-Aldrich) in 50 mM Tris-HCl, pH 7.4, 50 mM NaCl, 0.5 mM DTT. GST-USP8$_{542\text{-}1080}$ was then dialyzed at 4°C against 50 mM Tris-HCl, pH 7.4, 50 mM NaCl, 0.5 mM DTT, and 10% (v/v) glycerol; GST-USP8$_{542–660}$, GST-USP8$_{1–438}$, and GST-USP8$_{1–133}$ were dialyzed against 80 mM Pipes, pH 6.9, 1 mM $MgCl_2$, 1 mM ethylene glycol tetraacetic acid (EGTA), 1 mM DTT, and 10% (v/v) glycerol. Protein concentration was determined using the Bio-Rad DC protein assay. The purity of the GST-fused proteins was evaluated by SDS-PAGE and Coomassie Blue staining. If necessary, the purified proteins were concentrated with Centricon (Millipore, Billerica, MA). GST-USP8$_{542–660}$, GST-USP8$_{1–438}$, and GST-USP8$_{1–133}$ were ultracentrifuged with the TLA-100 rotor (Beckman Instruments, Palo Alto, CA) at 100 000 × *g* for 45 min, 4°C, before use.

Pull-down and Binding Assays

For pull-down experiments, 1% Triton X-100-soluble protein lysate (180 μg) from freshly isolated spermatids was incubated with 5 μg of purified GST-USP8$_{542\text{-}1080}$ or GST alone for 2 h at 4°C, followed by 1 h of incubation with glutathione-Sepharose beads. The beads were washed three times with washing buffer (50 mM Tris, pH 7.8, 100 mM NaCl, and 1 mM EDTA containing 0.1% Triton X-100, final concentration, and 10 μg each of leupeptin and aprotinin per milliliter) and once with washing buffer minus Triton X-100 before elution in SDS-PAGE sample buffer. Equal amounts of samples were resolved by SDS-PAGE and analyzed by Western immunoblotting.

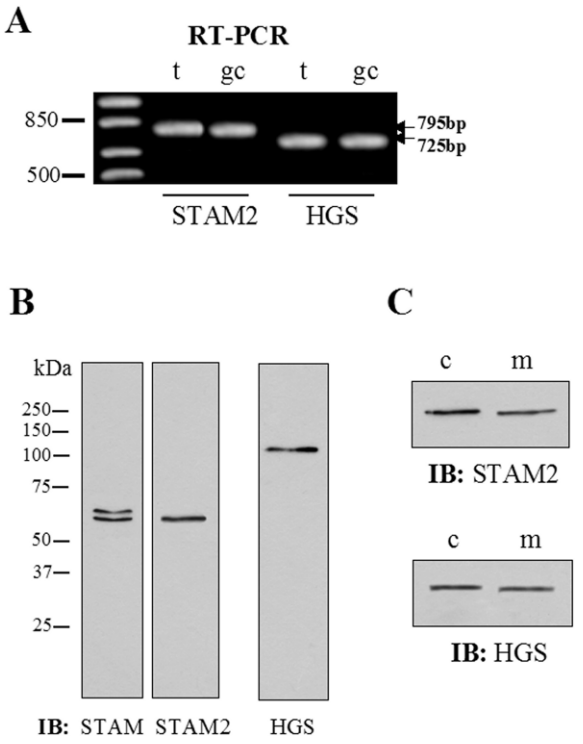

FIG. 1. Evidence for HGS and STAM2 in spermatogenic cells. **A**) The 795-bp transcript of mouse STAM2 and the 725-bp transcript of mouse HGS were detected by RT-PCR analysis in both testis (t) and isolated germ cells (gc). **B**) Immunoblots (IB) of 1% Triton X-soluble spermatogenic cell extract (75 μg) probed with (left) anti-STAM2 antibody (STAM = commercial anti-STAM; STAM2 = anti-STAM2 from Dr. Kitamura) and (right) anti-HGS antibody. **C**) Subcellular protein partition of spermatogenic STAM2 and HGS. Equal amounts of proteins (50 μg) from the cytosolic fraction (c) and membrane particulate fraction (m) of the hypotonic extract were immunoblotted against the indicated antibodies.

For binding assays, microtubules were prepared from pure mouse brain tubulin according to the protocol described by the manufacturer (Cytoskeleton, Denver, CO). Purified GST-USP8$_{542–660}$, GST-USP8$_{1–438}$, and GST-USP8$_{1–133}$ were incubated with preassembled, taxol-stabilized pure microtubules for 30 min at 25°C in a final volume of 50 μl 80 mM Pipes, pH 6.9, 1 mM $MgCl_2$, 1 mM EGTA, 0.5 mM DTT, 1 mM GTP, in the presence of 20 μM taxol. Bovine serum albumin (BSA), provided as a negative control in the manufacturer kit, was used in parallel. Pellets and supernatants, collected after centrifugation (30 000 × *g*, 45 min, 25°C) were separated by SDS-PAGE and analyzed by Western immunoblotting.

Microtubule Cosedimentation Assay

In vitro microtubule assembly was performed as described [36, 37]. Brain and testes from adult male CD1 mice were mechanically homogenized in 0.1 M Pipes, pH 6.9, 2 mM EGTA, 1 mM $MgSO_4$, 1 mM DTT, and 0.5 mM GTP supplemented with protease inhibitor cocktail (Sigma-Aldrich) at a ratio of 1 ml per g of tissue. The homogenates were first centrifuged at low speed (1000 × *g*, 10 min, 4°C) and then at high speed (100 000 × *g*, 60 min, 4°C). The collected supernatants (inputs) were incubated at 37°C for 30 min in the presence of 20 μM taxol, loaded on a 13% (w/v) sucrose cushion in the above buffer, and centrifuged at 45 000 × *g*, for 30 min at 30°C. Supernatants were then collected and supplemented with 4X SDS sample buffer, while the pellets were carefully resuspended in SDS sample buffer in the same total volume as the respective supernatant. Inputs and equal volumes of the supernatants and pellets were separated by SDS-PAGE and blotted on nitrocellulose membranes to be immunoprobed with anti-β-tubulin and anti-mouse USP8 antibodies.

Immunofluorescence

For immunohistochemistry, paraformaldehyde-fixed, paraffin-embedded testis sections (4 μm thick) were deparaffinized, blocked in 3% BSA, and incubated with primary antibodies at the appropriate dilution to be then visualized using Alexa Fluor 488-conjugated IgGs secondary antibodies (Invitrogen). Nuclei counterstaining was carried out with 2 μg/ml 4′-6-diamidino-2-phenylindole (DAPI, Sigma-Aldrich).

For immunocytochemistry, freshly prepared germ cell suspensions were processed for immunofluorescence analysis as previously described [33]. Briefly, 4% paraformaldehyde-fixed, ice-cold acetone-postfixed, preblocked spermatogenic cells were immunostained with the indicated primary antibodies, that is, anti-mouse USP8 (dilution 1:300), anti-STAM2 (1:100), anti-HGS (1:75), anti-VPS54 (1:100), anti-EEA1 (1:150), anti-β-tubulin (1:125), for 1 h at 37°C followed by their appropriate Alexa 488- or Alexa 568-conjugated secondary antibodies. In control samples, primary antibodies were omitted. Nuclei were counterstained with 2 μg/ml DAPI. Testis sections and isolated cells were examined on a Nikon Eclipse E 600 microscope equipped with filter sets for green (Alexa 488), red (Alexa 568), and blue (DAPI) fluorescence, and images were acquired with a Leica DG350F CCD camera (Leica Microsystems, Deerfield, IL) by using MS Imaging software. For simultaneous double immunolabeling, cells were examined also on a Leica TCS SP2AOBS confocal laser scanning microscope equipped with laser Ar/Kr (488 nm), laser He/Ne (568 nm), and laser UV (361–365 nm) for green, red, and blue fluorescence, respectively, and acquired by a computerized system (Leica Confocal Software). Sorted cells were identified according to their cellular size and nuclear shape according to the procedure outlined by O'Carroll et al. [38]. Images were elaborated with Adobe Photoshop 7.0 software (Mountain View, CA).

RESULTS

The ESCRT-0 Components STAM2 and HGS in Spermatogenic Cells

USP8 was identified as a protein interacting with the SH3 domain of STAM2 by a Far-Western screening of a mouse cDNA library [2]. STAM2 on its own was identified as the protein that interacts with HGS (hepatocyte growth factor-regulated tyrosine kinase substrate) [31]; STAM2 and HGS give rise to ESCRT-0 (endosomal-sorting complex required for transport-0). ESCRT-0 has the key function of initially recognizing ubiquitinated transmembrane cargo for protein sorting [39]; in addition, ESCRT-0, in combination with ESCRT-I, -II, and -III, imparts directionality to the endosomal-sorting machinery [35, 40]. We searched for STAM2 and its binding partner HGS in testis germ cells. Using selected primers specific to sequences of mouse STAM2 and HGS, the expected transcripts of 795 bp for STAM2 and of 725 bp for HGS were detected not only in testis RNA, but also in RNA extracted from isolated spermatogenic cells (Fig. 1A). To obtain evidence for the presence of HGS and STAM2 as proteins, spermatogenic cell protein lysates were subjected to immunoblotting analyses. HGS was detected utilizing a commercial HGS-antibody as a single band of 110 kDa, in agreement with the molecular weight reported by Komada and Kitamura [41] (Fig. 1B); STAM2 was recognized as a single band of 67 kDa by the STAM2-antibody developed by Takata et al. [31], while a commercial STAM-antibody yielded a double band of 67 kDa and 70 kDa (Fig. 1B). The 70-kDa immunoreactive band is likely due to the STAM isoform known as STAM1, which has a molecular weight slightly higher than STAM2. The subcellular protein fractionation into cytosolic and membrane fractions revealed that STAM2 and HGS could be recovered in both fractions (Fig. 1C); this finding indicates that the association between HGS and STAM2 could occur both in the cytosol and on membranes, in agreement with the role of ESCRT-0 proteins as selective cytosolic adaptors for recruiting ubiquitinated cargo to the early endosomes [39].

Cellular Distribution of STAM2 and HGS

Because the homogenates assayed by Western blot were proteins from the heterogeneous (meiotic and postmeiotic)

population of testicular spermatogenic cells, we analyzed the presence and localization of STAM2 and HGS by immunocytochemistry on fluorescently immunolabeled isolated testicular germ cells. Sorted cells were identified according to their cellular size and nuclear shape [38]. STAM2 was found to be characterized by puntuated cytosolic labeling in spermatocytes as well as in round spermatids (Fig. 2A). The puncta correspond to early endosomes as judged by colocalization of STAM2 with EEA1 (early endosomal antigen 1), an early endosomal marker, in double immunolabeled cells (Fig. 2B). HGS staining was also highly associated with punctuated vesicles in spermatocytes as well as in spermatids (Fig. 2C), and HGS/EEA1 immunopositivities colocalized on vesicles, sometimes forming a cluster (Fig. 2D). Double STAM2/HGS immunolabeling showed a strong colocalization of the two ESCRT-0 proteins (Fig. 2E). Altogether, these findings indicate that at least a portion of endogenous ESCRT-0 complexes is associated with the early endosome membranes of testicular germ cells.

USP8, STAM2, and HGS in Acrosomogenesis

When over-expressed ectopically, USP8 exhibits a cytoplasmic localization that is not characteristic of any single organelle [5]. Conversely, in spermatozoa, endogenous USP8 is not easily solubilized and associates with the cytosolic side of the acrosomal membrane and with the centrosome [11, 42]. The biogenesis of the acrosome is a multistep process that involves poorly understood events, including vesicular traffic and organelle migration [22, 23, 26, 30, 34]. To assess whether there is a link between acrosome biogenesis and membrane trafficking events proper of the early endosome compartment, our experimental plan was 1) to determine if USP8 associates with STAM2 and 2) to verify whether in differentiating spermatids the endocytic route with the early endosome as the major protein sorting hub develops into the acrosome.

By a pull-down assay, endogenous STAM2 was shown to be able to interact with USP8. The lower panel in Figure 3 shows that STAM2 was recovered in the precipitated recombinant USP8-protein complex, whereas it was not recovered in the control precipitated GST-protein complex. Association of STAM2 with a binding partner via the SH3 domain is considered essential for STAM2 function [2]. To localize STAM2 and USP8 in germ cells of intact testis, tissue sections were analyzed by immunofluorescence. Immunohistochemistry (Supplemental Fig. S1; all supplemental data are available online at www.biolreprod.org) confirmed that in diploid/meiotic cells STAM2 is characterized by a diffuse punctuate immunostaining exhibited also, although at a lower extent, by USP8. In testicular spermatids at steps 7–8, corresponding to the late cap phase/early acrosome phase, both STAM2 and USP8, however, accumulated markedly in the developing acrosome (Supplemental Fig. S1). USP8 and STAM2 were thus analyzed in isolated differentiating spermatids by simultaneous double immunolabeling and examined by the confocal microscopy. A discrete overlap between the two immunoreactivities (USP8, red; STAM2, green) was evidenced as yellow signals in the merged images (Fig. 3, upper panel). In particular, in elongating/elongated spermatids with a developed acrosome, USP8/STAM2 stainings superimposed, defining finely the profile of the acrosomal vacuole (Fig. 3, middle strip). Acrosome surface was also EEA1-immunopositive, and double USP8/EEA1 immunolabeling revealed USP8/EEA1-labeled punctuated structures on the acrosomal surface (Fig. 3, lower strip). Moreover, both ESCRT-0 components were found to label the surface of the developing acrosome as shown in Figure 4, upper strip; such immunopositivity was maintained up to the latest step of spermiogenesis with a considerable overlapping of HGS/STAM2 immunoreactivities on the acrosomal membrane of testicular spermatozoa (Fig. 4, lower strip). Taken together, the experimental evidence indicates that early endosome machinery takes part in the constitution of the sperm acrosome.

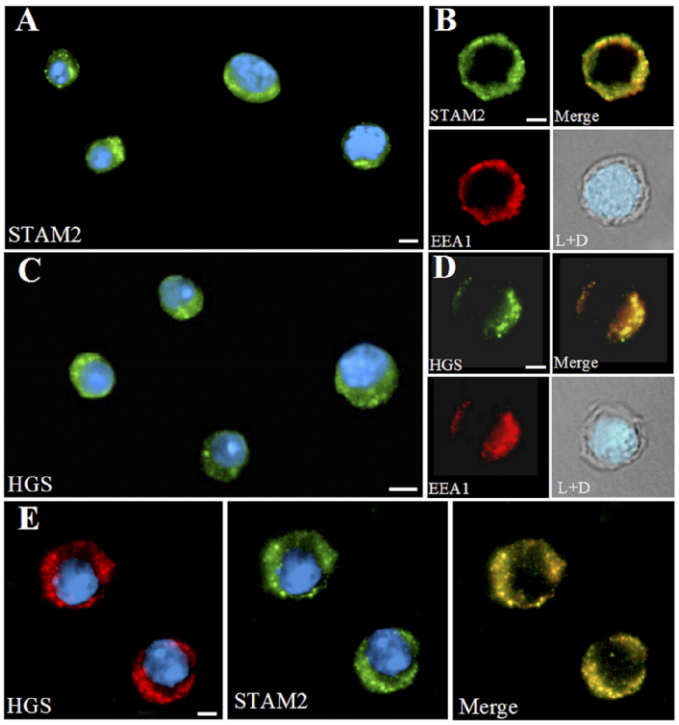

FIG. 2. Localization of STAM2 and HGS and their recruitment to early endosomes in spermatogenic cells. Both STAM2 (**A**) and HGS (**C**) show a diffuse cytoplasmic labeling characterized by punctuated, scattered vesicles in meiotic and postmeiotic round cells. STAM2-positive (**B**) and HGS-positive (**D**) vesicles correspond to early endosomes as judged in the merged images of the double STAM2 (green)/EEA1 (red) and HGS (green)/EEA1 (red) immunolabelings; L+D = merged light and DAPI images. **E**) The double HGS (red)/STAM2 (green) immunolabeling shows the strong colocalization of the two ESCRT-0 components on early endosomes of spermatogenic cells. Nuclei are stained with DAPI. Yellow fluorescence in the merged images indicates colocalization. Bars = 7 μm (**A** and **C**) and 4 μm (**B**, **D**, and **E**).

VPS54 in Spermatogenic Cells

Selective transport between organelles requires that transport intermediates be targeted to appropriate downstream compartments; tethering complexes must therefore recognize membrane-associated factors on both the donor and recipient compartments. Vacuolar protein sorting 54 (VPS54) is a component of the so-called Golgi-associated retrograde protein (GARP)-tethering complex that in mammalian cells is formed by VPS52, VPS53, and VPS54 [32]. In particular, VPS54 is selectively required for the retrograde transport from early endosomes; moreover, different domains of VPS54 confer separate functions to the protein [43]. Whereas the N-terminus is important for VPS54 assembly and stability of the GARP complex, the C-terminus, which is evolutionarily conserved, is essential to mediate VPS54 localization to the early endosome [43]. A C-terminus point mutation of *Vps54* mouse gene, namely VPS54(L967Q), is known to be the responsible for the wobbler mouse phenotype [44], characterized by motor neuron

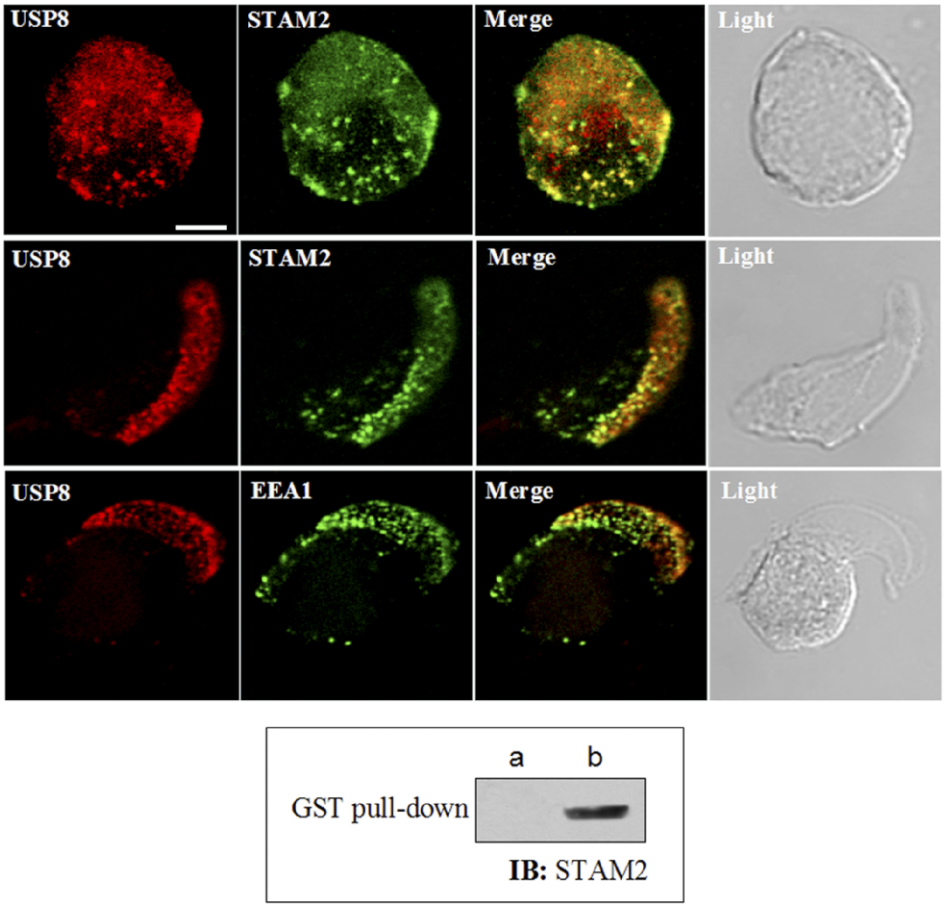

FIG. 3. USP8-STAM2 protein interaction during acrosomogenesis. Upper panel, endogenous USP8 (red) colocalizes with endogenous STAM2 (green). In spermatids at the Golgi phase (steps 1–3, upper strip), when proacrosomic granules are developing, USP8/STAM2 double-labeled vesicles are present mainly in a restricted, polarized region at the periphery of the nucleus. In condensing spermatids (steps 13–14, middle strip), USP8 and STAM2 immunostainings, respectively, mark the profile of the fully formed acrosomal vesicle; several puncta of USP8/STAM2 colocalization result in the merged image. The acrosomal membrane shows EEA1 immunopositivity even in condensing spermatids, with discrete spots of USP8/EEA1 colocalization (lower strip). Bar = 4 μm in upper strip and 6 μm in middle and lower strips. Lower panel, USP8-STAM2 protein interaction. GST pull-down of spermatid protein lysate incubated with control GST (a) or GST-$USP8_{542-1080}$ (b) then immunoblotted with STAM2 antibody; spermatid STAM2 is recovered only in the GST-$USP8_{542-1080}$ precipitate.

degeneration and defective spermiogenesis. The male fertility disorder is due to the production of spermatozoa lacking a real acrosome (for a review, see [45]). Notwithstanding this, VPS54 has not yet been studied in male germ cells. So, we searched for the presence of VPS54 in testicular germ cells, focusing attention on differentiating spermatids. A protein of 130 kDa was specifically recognized in a VPS54-immunoblotting assay of protein lysates (Fig. 5A). Immunofluorescence analyses provided information about VPS54 localization in spermatogenic germ cells. Immunocytochemistry revealed that in spermatocytes and early round spermatids VPS54 exhibits a rather diffuse spotted distribution inside the cytoplasm (Fig. 5B); in later round spermatids, however, VPS54 was found to be concentrated at the developing acrosomal cap, and, as acrosomogenesis proceeds, it became evident as a markedly dotted labeling of the acrosome surface until its full development (Fig. 5B). Moreover, immunohistochemistry demonstrated VPS54 labeling of the crescent-shaped acrosome in differentiating spermatids (Fig. 5C); this VPS54 immunostaining is highly reminiscent of those immunorevealed with anti-USP8 and anti-STAM2 (Supplemental Fig. S1). We performed also double VPS54/STAM2 and VPS54/USP8 immunolabelings to check for possible direct colocalization at the confocal microscope. VPS54/STAM2 colocalization was immunorevealed on spermatid vesicle structures (Supplemental Fig. S2); moreover, in spermatids developing the acrosome, yellow spots of VPS54/USP8 superimposition were observed in the acrosome area (Supplemental Fig. S3). It follows that VPS54 behaves differently from Golgi-associated anterograde transport proteins that associate with the developing acrosome only at the early step of acrosomogenesis to be then discharged [22, 34]. VPS54, on the contrary, follows the route of the USP8 and ESCRT-0 complex until full acrosomal maturation, suggesting that VPS54 could work in cooperation with the spermatid's early endosome machinery in the biogenesis of the acrosome.

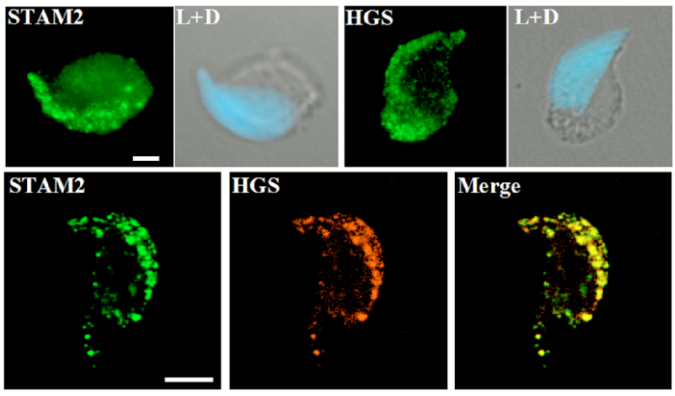

FIG. 4. STAM2 and HGS localization in acrosome-developing spermatids and testicular spermatozoa. Upper strip: single STAM2 and HGS immunolabelings in elongating spermatids (steps 9–12) show the strong compartmentalization of the two ESCRT-0 components in the acrosomal region; L+D, merged light and DAPI images. Lower strip: the acrosomal surface of testicular spermatozoa is still characterized by a marked STAM2/HGS colocalization as indicated by the superimposition of the double immunostaining. Bars = 5.5 μm.

USP8 and Microtubules

Endocytic vesicles migration is linked to microtubules [46], and assembly of the acrosome is known to be dependent on

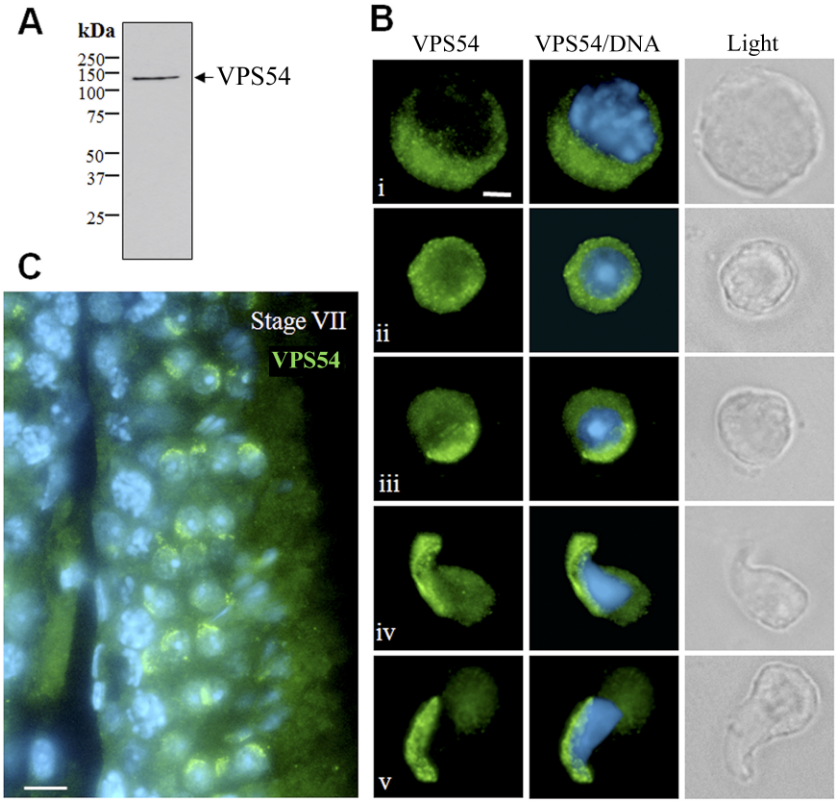

FIG. 5. VPS54 in spermatogenic cells. VPS54 was immunorevealed with the rabbit polyclonal VPS54 antibody. **A**) VPS54 immunoblot of a spermatogenic cell lysate; these cells are VPS54 positive and express a VPS54 of estimated 130 kDa, in agreement with the protein prediction. **B**) VPS54 localization in different types of spermatogenic cells: i, a primary spermatocyte; ii, an early round spermatid; iii, a cap-phase spermatid; iv, an elongating spermatid; v, a condensing spermatid. Bar = 5.5 μm. **C**) VPS54 was localized in fixed adult testis (4 μm sections), and DNA was stained with DAPI; VPS54 at stage VII of the epithelial cycle was found as punctuated spots associated with the flattened developing acrosome in step 7 spermatids. Bar = 19 μm.

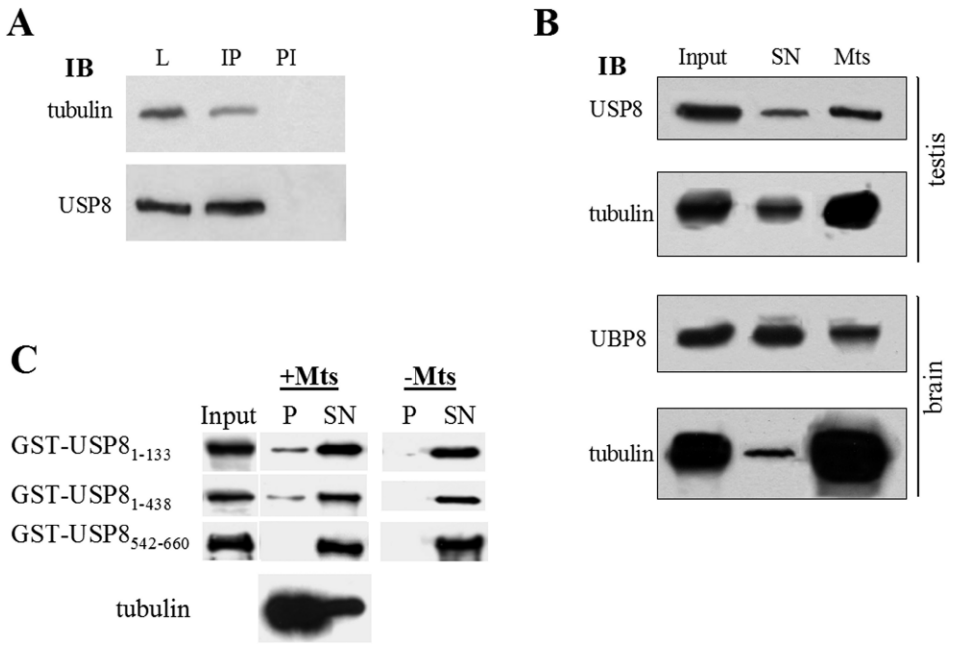

FIG. 6. USP8 binds to microtubules. **A**) Coimmunoprecipitation of endogenous proteins. Spermatogenic cell lysate (L) was immunoprecipitated with antibodies against USP8 (IP) or, as a control, preimmune serum (PI). Immunoprecipitates, separated by SDS-PAGE, were immunoblotted (IB) with antibodies against β-tubulin (upper strip) and against USP8 (lower strip). **B**) Endogenous USP8 cosediments with in vitro assembled microtubules. Cytosolic high-speed supernatants of mouse testis and brain homogenates (Input) were incubated in the presence of 20 μM taxol and then loaded on a sucrose cushion to be sedimented by centrifugation. The microtubule pellets (Mts), supernatants (SN), and Inputs, resolved by SDS-PAGE, were analyzed against both USP8 and tubulin antibodies. **C**) MIT domain of USP8 binds directly to microtubules. Different USP8 fusion proteins were used for in vitro microtubule-binding assays. Specifically, purified GST-USP8$_{1–133}$, GST-USP8$_{1–438}$, and GST-USP8$_{542–660}$ were incubated with (+) or without (-) pure preassembled microtubules (Mts) as described in *Materials and Methods*. Inputs, pellets (P), and supernatants (SN) were analyzed by Western immunoblotting with antibodies to GST (the three upper strips) and β-tubulin (lowest strip).

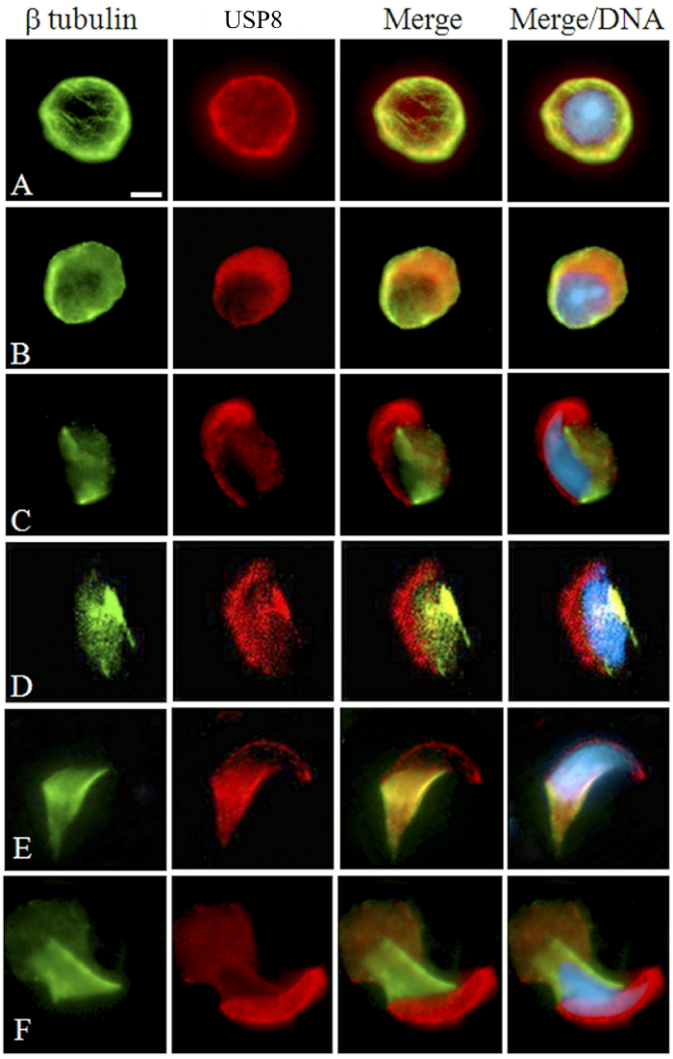

FIG. 7. USP8 localizes to microtubules during acrosomogenesis. In all cases, endogenous USP8 is visible as a red signal; microtubules are revealed using a monoclonal antibody against β-tubulin, green signal; nuclei are stained with DAPI, blue signal. Colocalization is indicated by yellow signal in merged image. **A**) An early round spermatid that exhibits the characteristic cortical microtubule network to which USP8 staining frequently overlaps. **B**) In late rounds spermatids, there is an increase, on the one hand, of β-tubulin immunostaining around the surface of the nucleus that is starting to elongate and, on the other hand, of USP8 immunostaining on the developing acrosomal vacuole. The two immunostainings, however, still overlap in discrete areas as at the equatorial segment. **C** and **D**) In elongating spermatids with a developed acrosome, at superficial focal planes (**C**) USP8 (dorsal side) is apparently positioned opposite to the microtubular manchette (ventral side); deeper focal planes (**D**), however, reveal a considerable USP8/β-tubulin overlapping positioned just at the level of the manchette at the ventral side of the spermatid head. **E**) In condensing spermatids, consistent with the descent of the manchette, β-tubulin stains the posterior region of the head; USP8 immunolabeling, however, still superimposes on the manchette. **F**) In spermatids where the manchette is about to disassemble, USP8 marks predominantly the acrosomal region. Bar = 5 μm.

microtubules [23]. We found previously that mouse USP8 is able to interact in vitro with γ-tubulin [42] while a more recent study [35] has identified by in silico analysis an MIT domain at the amino-terminus of USP8. In transfected cells, an MIT-deleted *USP8* mutant is unable to localize on endosomes and to rescue its binding partner STAM2 from proteasomal degradation [35]. An MIT domain has been so far identified in a few proteins such as VPS4, SNX15, spartin, and spastin [47]; notably, all these proteins have a well established role in endosomal trafficking. We searched for a putative link between endogenous USP8 and microtubules during acrosomogenesis/sperm head morphogenesis. First, USP8/β-tubulin coimmunoprecipitation assays were carried out to test whether USP8 and tubulin interact in mouse spermatogenic cells. The USP8 immunoprecipitate, first resolved by SDS-PAGE, yielded a positive signal when it was immunoblotted against β-tubulin antibodies (Fig. 6A). To get an insight on a possible association of USP8 with microtubules, further investigation was carried out on polymerized tubulin through cosedimentation assays where both mouse testis and brain homogenates were analyzed. Brain was utilized for two reasons: 1) brain serves as a standardized positive control for checking the presence of microtubules, and 2) it is the other elective tissue for USP8 expression. Microtubules were assembled when testis and brain high-speed supernatants (Inputs) were incubated at 37°C for 30 min in the presence of the microtubule-polymerizing agent taxol [36, 37]. Microtubules and linked proteins were isolated by sedimentation through a sucrose cushion. The microtubule pellets, resuspended in the same volume as the supernatants, and an equal volume of Inputs were resolved by SDS-PAGE and analyzed by Western blotting using antibodies against both USP8 and tubulin. Figure 6B shows that a consistent amount of testicular and brain USP8 present in the input fractions cosedimented with the microtubules. Finally, to verify whether the USP8-microtubules association is direct, as other proteins present in the tissue extracts could mediate such an interaction, we investigated the association using pure proteins. Purified USP8 recombinant proteins containing the MIT domain (amino acids 1–133), that is, GST-USP8$_{1–133}$ and GST-USP8$_{1–438}$, were prepared and incubated with microtubules that were preassembled from pure commercial tubulin; both pellets and supernatants were then analyzed. Under these conditions, a discrete portion of both recombinant USP8 proteins was precipitated with the taxol-stabilized microtubules (Fig. 6C); no GST-USP8$_{1–133}$ or GST-USP8$_{1–438}$ was precipitated in the absence of microtubules (Fig. 6C). In contrast, GST-USP8$_{542–660}$, which does not contain the MIT domain and was used as a selective negative control, did not precipitate in the presence of taxol-stabilized microtubules (Fig. 6C). BSA, used as a standardized negative control, was not detected in the microtubule pellet (data not shown). These findings indicate that MIT-containing USP8 directly interacts with microtubules.

The next step in assessing the in vivo association of USP8 with microtubules was to check for protein colocalization using USP8 and β-tubulin antibodies during acrosomogenesis/sperm head morphogenesis. Spermatids, during their differentiation, exhibit two peculiar and transient microtubule arrays, namely, the cortical microtubule array of the early phase [23] and the manchette (steps 8–13 of spermiogenesis) (30). DAPI staining and epifluorescence were always employed for a careful identification of the nuclear structure and cell morphology, respectively. Figure 7 summarizes some significant findings. First, at the so-called Golgi phase when the acrosome starts to differentiate from peripherally located proacrosomic granules [34], both USP8 (red) and β-tubulin (green) label the cell periphery as a dense area; the overlay of the two immunostainings resulted in fair spots of yellow fluorescence, indicating that USP8- and β-tubulin-immunostained structures colocalized (Fig. 7A). Second, β-tubulin immunostaining of spermatids at step 8 shows the characteristic symmetric belt of microtubules of the developing manchette that will cover approximately half of the nucleus; on its own, USP8 spans predominantly the other half of the nucleus, consistent with the location of the developing acrosome. The superimposition of

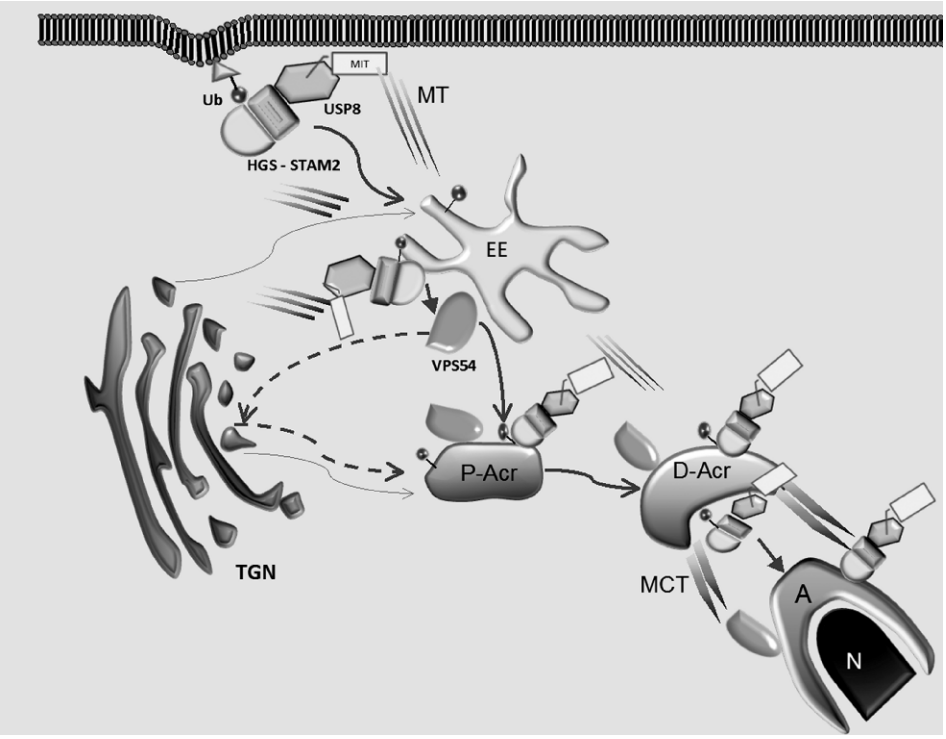

FIG. 8. Schematic representation of the endosomal pathway involved in the biogenesis of the acrosome. Ubiquitination (bound little ball) of a membrane/early vesicle protein serves as a sorting signal for its recruitment by the selected effectors HGS-STAM2 to the early endosome (EE). Here USP8 is also recruited via its interaction with STAM2; moreover, USP8, through its MIT domain, is responsible for the localization and microtubule (MT)-mediated transport of ubiquitinated protein cargo in endosomal sorting. The thick arrows depict the early endosomal route, and the thin arrows the Golgi-derived biosynthetic cargo (TGN) destined for acrosome biogenesis. EE is the protein-sorting center where the endosomal and biosynthetic pathways connect. Through the tethering factor VPS54, EE-derived vesicular cargo is transported (solid arrow, direct path; dashed arrows, indirect path) to the proacrosome (P-Acr) that evolves in the developing acrosome (D-Acr). During spermatid elongation, shaping of the acrosome (A) occurs via microtubular manchette (MCT); USP8, still complexed with interacting proteins on the acrosome surface, could mediate the shaping process through its MIT domain. n, nucleus.

the two immunostainings results, however, in some yellow spots of β-tubulin/USP8 colocalization (Fig. 7B). Third, at a later stage, the apparently opposite USP8 versus manchette positioning becomes more evident (Fig. 7C). Fourth, deeper focal planes, however, reveal a considerable overlap of USP8 and β-tubulin immunofluorescence as documented by the strong yellow signal at the ventral side of the cell, where the developed manchette is located (Fig. 7D). Finally, at more advanced differentiation steps, the manchette is extended into the distal cytoplasm or is about to disassemble while USP8 delineates the acrosome; a transient USP8/β-tubulin superimposition is, however, still visible (Fig. 7E).

DISCUSSION

Recently, considerable progress has been made in defining functional properties of USP8 in the regulation of endosomal protein sorting and endosome morphology using in vitro and cell culture systems. A physiological link between USP8 and endosomes in vivo is, however, still elusive. In this study, we provide evidence for a possible biological role of USP8, namely, its involvement in the endocytic pathway that culminates with the formation of the acrosome, an acidic vacuole unique to male germ cells.

The acrosome is highly conserved throughout evolution and is indispensable for fertilization in mammals [30]. The nature of the molecular machinery involved in acrosomogenesis and how the selective components interact with each other and are regulated in time and space remain an unsolved matter. Here we show that spermatogenic cells express HGS and STAM2, the two proteins that form the ESCRT-0 complex; these localize in both meiotic and postmeiotic cells on vesicles identified as early endosomes by costaining with EEA1. Ubiquitination of transmembrane proteins serves as a signal for sorting ubiquitinated proteins at various compartments of the endosomal/lysosomal system. HGS and STAM2, via their ubiquitin-interacting motifs, exert the initial key event, that is, they recognize and bind the ubiquitinated cargo, thereby internalizing it into the endocytic pathway [39]. The deubiquitinating enzyme USP8, recruited to the early endosome via interaction with STAM2, is a regulator of endosomal sorting by specifying the trimming or removal of the ubiquitin moiety bound to the selected itinerant cargo [5, 16]. In this study, endogenous STAM2 is shown to interact with the SH3-binding domain of USP8 and to colocalize with USP8 on early endosomes. So USP8, which is highly expressed in spermatogenic cells [3], can exert its regulatory function in a physiological context. Immunofluorescence analysis has revealed that in spermatids undergoing cytodifferentiation, ESCRT-0/USP8/EEA1-positive vesicles no longer exhibit the scattered distribution inside the cytoplasm found in meiotic and early round spermatids, but rather they significantly contribute to the development of the acrosomal vacuole.

Thus, the early endosome machinery of postmeiotic male germ cells is apparently engaged in the biogenesis of the acrosome; acrosomogenesis, however, seems to differ from the classical endosome-lysosome pathway. In protein sorting to the lysosomes, in fact, ubiquitins are removed from the protein cargo by the deubiquitinating enzymes USP8 and AMSH (associated molecule with the SH3 domain of STAM) so that the ESCRT complexes, and consequently the deubiquitinases, dissociate from the lysosome [7, 16, 40]. Conversely, in the present study, the limiting acrosomal membrane is found to maintain ESCRT-0/USP8/EEA1 immunoreactivities until full maturation of the vacuole. What emerges is that if the acrosome cannot be considered as a direct Golgi derivative, it cannot be thought of either as a canonical lysosome. Taking into account the present data and the previous ones in support of a direct Golgi derivation [19–21], a possible explanation is that both the endocytic pathway and the biosynthetic pathway are involved in acrosomogenesis just as they are in the biogenesis of lysosome-related organelles (LROs) [48]. LROs are membrane-bound cytoplasmic organelles restricted to certain specialized cell types, such as the melanosomes in melanocytes and lytic granules in lymphocytes. LROs share features with

lysosomes but have distinct morphology, composition, and/or functions. As reported by Huizing et al. [48], LRO biogenesis has the early endosome as the crucial protein-sorting hub in the cell. Golgi-derived biosynthetic cargo and/or late endosomes/lysosomes as well as receptors or other molecules internalized from the cell membrane are in fact sorted to the early endosome, which develops and evolves into the LRO [48]. Moreover, a possible involvement of retrograde traffic from early endosomes during acrosome biogenesis comes out from the data we obtained on the vesicle-trafficking protein VPS54. So far not yet studied in male germ cells, VPS54 has been found to follow the route of USP8/ESCRT-0 labeled vesicles in spermatids in the development of the acrosome. This finding is noteworthy also vis-à-vis understanding the wobbler male mice phenotype [44, 45].

Another significant finding in the present study is the relationship between USP8 and microtubules. Both acrosome [23] and LRO [48] biogenesis are microtubule-dependent. However, there is scanty information about how proacrosomal vesicles are mobilized during acrosome biogenesis [23, 30]. Our microtubule cosedimentation and binding assays provide the first biochemical evidence that USP8, through its MIT domain, is effective at binding microtubules. In addition, immunofluorescence analysis demonstrates that during acrosomogenesis endogenous USP8 colocalizes with spermatid microtubule structures, that is, the cortical microtubule array and the manchette. Thus, it emerges that USP8, in a physiological context, could play a double critical role: 1) that of a regulatory endosome-associated deubiquitinating enzyme and 2) that of a microtubule-interacting/transport protein capable of mediating directly the link between the sorted itinerant endocytic vesicle and microtubules. As a final observation of interest, we mention the association of USP8 with the manchette. This suggests a role for USP8 also in the shaping of the acrosome/sperm head, which has been attributed to CLIP1 (CAP-GLY domain-containing linker protein 1), a microtubule plus-end-tracking protein [49]. In cultured cells, CLIP1 is involved in the linking of endosomes to microtubules [50]; in spermatids, CLIP1 accumulates on manchettes and centrosomes while *Clip1* −/− male mice are subfertile since their sperm have abnormal heads [49].

On the basis of the present findings, we propose a schematic model for the biogenesis of the acrosome (Fig. 8), which is suggested to be a novel LRO. Of course, other molecular players are involved; these are yet unidentified and/or, even if in fact identified, may have been positioned not correctly in the acrosomogenetic route. What deserves particular attention will be the identification of the ubiquitinated membrane proteins selectively sorted and transported via their recruitment by the USP8-ESCRT-0/VPS54 system to the developing acrosome.

ACKNOWLEDGMENTS

We thank Dr. S. Urbé (School of Biomedical Sciences, Liverpool, U.K.) for providing the pGEX-GST-USP8$_{1–438}$ and pGEX-GST-USP8$_{1–133}$ plasmids and Dr. E. Martegani (Milano-Bicocca University, Italy) for the pGEX-GST-USP8$_{542-1080}$ plasmid. Thanks to Dr. N. Kitamura (Graduate School of Bioscience and Biotechnology, Tokyo Institute of Technology, Yokohama, Japan) and Dr. F. Stenner (Zurich Hospital, Switzerland) for supplying the rabbit anti-STAM2 and anti-VPS54 antibodies, respectively.

REFERENCES

1. Naviglio S, Matteucci C, Matoskova B, Nagase T, Nomura N, Di Fiore PP, Draetta GF. UBPY: a growth-regulated human ubiquitin isopeptidase. EMBO J 1998; 17:3241–3250.
2. Kato M, Miyazawa K, Kitamura N. A deubiquitinating enzyme UBPY interacts with the Src homology 3 domain of Hrs-binding protein via a novel binding motif PX(V/I)(D/N) RXXKP. J Biol Chem 2000; 275: 37481–37487.
3. Gnesutta N, Ceriani M, Innocenti M, Mauri I, Zippel R, Sturani E, Borgonovo B, Berruti G, Martegani E. Cloning and characterization of mouse UBPY, a deubiquitinating enzyme that interacts with the ras guanine nucleotide exchange factor CDC25(Mm)/Ras-GRF1. J Biol Chem 2001; 276:39448–39454.
4. Amerik AY, Nowak J, Swaminathan S, Hochstrasser M. The Doa4 deubiquitinating enzyme is functionally linked to the vacuolar protein-sorting and endocytic pathways. Mol Biol Cell 2000; 11:3365–3380.
5. Mizuno E, Iura T, Mukai A, Yoshimori T, Kitamura N, Komada M. Regulation of epidermal growth factor receptor down-regulation by UBPY-mediated deubiquitination at endosomes. Mol Biol Cell 2005; 16: 5163–5174.
6. Row PE, Prior IA, McCullough J, Clague MJ, Urbe S. The ubiquitin isopeptidase UBPY regulates endosomal ubiquitin dynamics and is essential for receptor down-regulation. J Biol Chem 2006; 281:12618–12624.
7. Alwan HA, van Leeuwen JE. UBPY-mediated epidermal growth factor receptor (EGFR) de-ubiquitination promotes EGFR degradation. J Biol Chem 2007; 19:1658–1669.
8. Mizuno E, Kobayashi K, Yamamoto A, Kitamura N, Komada M. A deubiquitinating enzyme UBPY regulates the level of protein ubiquitination on endosomes. Traffic 2006; 7:1017–1031.
9. Niendorf S, Oksche A, Kisser A, Lohler J, Prinz M, Schorle H, Feller S, Lewitzky M, Horak I, Knobeloch KP. Essential role of ubiquitin-specific protease 8 for receptor tyrosine kinase stability and endocytic trafficking in vivo. Mol Cell Biol 2007; 27:5029–5039.
10. Nijman SM, Luna-Vargas MP, Velds A, Brummelkamp TR, Dirac AM, Sixma TK, Bernards R. A genomic and functional inventory of deubiquitinating enzymes. Cell 2005; 123:773–786.
11. Berruti G, Martegani E. The deubiquitinating enzyme mUBPY interacts with the sperm-specific molecular chaperone MSJ-1: the relation with the proteasome, acrosome, and centrosome in mouse male germ cells. Biol Reprod 2005; 72:14–21.
12. Bruzzone F, Vallarino M, Berruti G, Angelini C. Expression of the deubiquitinating enzyme mUBPY in the mouse brain. Brain Res 2008; 1195:56–66.
13. Haglund K, Dikic I. Ubiquitylation and cell signaling. EMBO J 2005; 24: 3353–3359.
14. Wang J, Wang CE, Orr A, Tydlacka S, Li SH, Li XJ. Impaired ubiquitin proteasome system activity in the synapses of Huntington's disease mice. J Cell Biol 2008; 180:1177–1189.
15. Kierszenbaum AL. Intramanchette transport (IMT): managing the making of the spermatid head, centrosome, and tail. Mol Reprod Dev 2002; 63: 1–4.
16. Clague MJ, Urbè S. Endocytosis: the DUB version. Trends Cell Biol 2006; 16:551–559.
17. Cosker KE, Courchesne SL, Segal RA. Action in the axon: generation and transport of signaling endosomes. Curr Opin Neurobiol 2008; 18:270–275.
18. Hartree EF. The acrosome-lysosome relationship. J Reprod Fertil 1975; 44:125–126.
19. Tang XM, Lalli MF, Clermont Y. A cytochemical study of the Golgi apparatus of the spermatid during spermiogenesis in the rat. Am J Anat 1982; 163:283–294.
20. Burgos MH, Gutierrez LS. The Golgi complex of the early spermatid in guinea pig. Anat Rec 1986; 216:139–145.
21. Martinez MJ, Geuze HJ, Ballesta J. Evidence for a nonlysosomal origin of the acrosome. J Histochem Cytochem 1996; 44:313–320.
22. Moreno RD, Ramalho-Santos J, Chan EK, Wessel GM, Schatten G. The Golgi apparatus segregates from the lysosomal/acrosomal vesicle during rhesus spermiogenesis: structural alterations. Dev Biol 2000; 219:334–349.
23. Moreno RD, Palomino J, Schatten G. Assembly of spermatid acrosome depends on microtubule organization during mammalian spermiogenesis. Dev Biol 2006; 293:218–227.
24. Sun-Wada GH, Imai-Senga Y, Yamamoto A, Murata Y, Hirata T, Wada Y, Futai M. A proton pump ATPase with testis-specific E1-subunit isoform required for acrosome acidification. J Biol Chem 2002; 277: 18098–18105.
25. Moreno RD, Alvarado CP. The mammalian acrosome as a secretory lysosome: new and old evidence. Mol Reprod Dev 2006; 73:1430–1434.
26. Li Y-C, Hu X-Q, Zhang K-Y, Guo J, Hu Z-Y, Tao S-X, Xiao L-J, Wang Q-Z, Han C-S, Liu X-L. Afaf, a novel vesicle membrane protein, is related to acrosome formation in murine testis. FEBS Letter 2006; 580:4266–4273.

27. Li S, Qiao Y, Di Q, Le X, Zhang L, Zhang X, Zhang C, Cheng J, Zong S, Koide SS, Miao S, Wang L. Interaction of SH3P13 and DYDC1 protein: a germ cell component that regulates acrosome biogenesis during spermiogenesis. Eur J Cell Biol 2009; 88:509–520.
28. Zhu G, Salazar G, Zlatic SA, Fiza B, Doucette MM, Heilman CJ, Levey AJ, Faundez V, L'Hernault SW. SPE-39 family proteins interact with the HOPS complex and function in lysosomal delivery. Mol Biol Cell 2009; 20:1223–1240.
29. West AP, Willison KR. Brefeldin A and mannose 6-phosphate regulation of acrosomic related vesicular trafficking. Eur J Cell Biol 1996; 70:315–321.
30. Kierszenbaum AL, Tres L. The acrosome-acroplaxome-manchette complex and the shaping of the spermatid head. Arch Histol Cytol 2004; 67: 271–284.
31. Takata H, Kato M, Denda K, Kitamura N. A HGS binding protein having a Src homology 3 domain is involved in intracellular degradation of growth factors and their receptors. Genes Cells 2000; 5:57–69.
32. Liewen H, Meinhold-Heerlein I, Oliveira V, Schwarzenbacher R, Luo G, Wadle A, Jung M, Pfreundschuh M, Stenner-Liewen F. Characterization of the human GARP (Golgi associated retrograde protein) complex. Exp Cell Res 2005; 306:24–34.
33. Aivatiadou E, Ripolone M, Brunetti F, Berruti G. cAMP-Epac2-mediated activation of Rap1 in developing male germ cells: RA-RhoGAP as a possible direct down-stream effector. Mol Reprod Dev 2009; 76:407–416.
34. Moreno RD, Ramalho-Santos J, Sutovsky P, Chan EK, Schatten G. Vesicular traffic and Golgi apparatus dynamics during mammalian spermatogenesis: implications for acrosome architecture. Biol Reprod 2000; 63:89–98.
35. Row PE, Liu H, Hayes S, Welchman R, Charalabous P, Hofmann K, Clague MJ, Sanderson CM, Urbé S. The MIT domain of UBPY constitutes a CHMP binding and endosomal localisation signal required for efficient EGF receptor degradation. J Biol Chem 2007; 282:30929–30937.
36. Forlani G, Baldassa S, Lavagni P, Sturani E, Zippel R. The guanine nucleotide exchange factor RasGRF1 directly binds microtubules via DHPH2-mediated interaction. FEBS J 2006; 273:2127–2138.
37. Vallee RB. Purification of brain microtubules and microtubule-associated protein 1 using taxol. Methods Enzymol 1986; 134:104–115.
38. O'Carroll D, Scherthan H, Peters AHFM, Opravil S, Haynes AR, Laible G, Rea S, Schmid M, Lebersorger A, Jerratsch M, Sattler L, Mattei MG, et al. Isolation and characterization of Suv39h2, a second histone H3 methyltransferase gene that displays testis-specific expression. Mol Cell Biol 2000; 20:9423–9433.
39. Hicke L, Dunn R. Regulation of membrane protein transport by ubiquitin and ubiquitin-binding proteins. Annu Rev Cell Dev Biol 2003; 19:141–172.
40. Tanaka N, Kyuuma M, Sugamura K. Endosomal sorting complex required for transport proteins in cancer pathogenesis, vesicular transport, and non-endosomal functions. Cancer Sci 2008; 99:1293–1303.
41. Komada M, Kitamura N. The Hrs/STAM complex in the downregulation of receptor tyrosine kinases. J Biochem 2005; 137:1–8.
42. Berruti G, Aivatiadou E. mUBPY is a novel centrosome-associated protein and interacts with gamma-tubulin. J Submicrosc Cytol Pathol 2006; 38: 77–83.
43. Quenneville NR, Chao TY, McCaffery JM, Conibear E. Domains within the GARP subunit Vps54 confer separate functions in complex assembly and early endosome recognition. Mol Biol Cell 2006; 17:1859–1870.
44. Schmitt-John T, Drepper C, Mussmann A, Hahn P, Kuhlmann M, Thiel C, Hafner M, Lengeling A, Heimann P, Jones JM, Meisler MH, Jockusch H. Mutation of VPS54 causes motor neuron disease and defective spermiogenesis in the wobbler mouse. Nat Genet 2005; 37:1213–1215.
45. Boillée S, Peschanski M, Junier MP. The wobbler mouse: a neurodegeneration jigsaw puzzle. Mol Neurobiol 2003; 28:65–106.
46. Apodaca G. Endocytic traffic in polarized epithelial cells: role of the actin and microtubule cytoskeleton. Traffic 2001; 2:149–159.
47. Ciccarelli FD, Proukakis C, Patel H, Cross H, Azam S, Patton MA, Bork P, Crosby AH. The identification of a conserved domain in both spartin and spastin, mutated in hereditary spastic paraplegia. Genomics 2003; 81: 437–441.
48. Huizing M, Helip-Wooley A, Westbroek W, Gunay-Aygun M, Gahl WA. Disorders of lysosome-related organelle biogenesis: clinical and molecular genetics. Annu Rev Genom Human Genet 2008; 9:359–386.
49. Akhmanova A, Mausset-Bonnefont AL, van Cappellen W, Keijzer N, Hoogenraad CC, Stepanova T, Drabek K, van der Wees J, Mommaas M, Onderwater J, van der Meulen H, Tanenbaum ME, et al. The microtubule plus-end-tracking protein CLIP-170 associates with the spermatid manchette and is essential for spermatogenesis. Genes Dev 2005; 19: 2501–2515.
50. Pierre P, Scheel J, Rickard JE, Kreis TE. CLIP-170 links endocytic vesicles to microtubules. Cell 1992; 70:887–900.